Research Square

Preprints are preliminary reports that have not undergone peer review.
They should not be considered conclusive, used to inform clinical practice,
or referenced by the media as validated information.

Combined Transcriptomic and WGCNA Analyses of Prohexadione- Calcium-Mediated Regulation of Shoot Growth in Greenhouse Peach

Yu Wang
Changli Institute of Pomology, Hebei Academy of Agriculture and Forestry Sciences,
Yonghong Li
Changli Institute of Pomology, Hebei Academy of Agriculture and Forestry Sciences,
Jie Li
Changli Institute of Pomology, Hebei Academy of Agriculture and Forestry Sciences,
Qihang Tian
Changli Institute of Pomology, Hebei Academy of Agriculture and Forestry Sciences,
Zhendong Tian
Changli Institute of Pomology, Hebei Academy of Agriculture and Forestry Sciences,
Ruifeng Chang
Changli Institute of Pomology, Hebei Academy of Agriculture and Forestry Sciences,
Guojian Liu
Changli Institute of Pomology, Hebei Academy of Agriculture and Forestry Sciences,
Zhaoyuan Wang
wy912963518@163.com

Changli Institute of Pomology, Hebei Academy of Agriculture and Forestry Sciences,

Article

Keywords: Prohexadione-calcium, Peach, Vegetative shoot growth, Transcriptomics, WGCNA

Posted Date: November 24th, 2026

DOI: https://doi.org/10.21203/rs.3.rs-11518613/v1

License: This work is licensed under a Creative Commons Attribution 4.0 International License.
Read Full License

Additional Declarations:
No competing interests reported.

Table 1 is available in the Supplementary Files section.

Combined Transcriptomic and WGCNA Analyses of Prohexadione-Calcium-Mediated Regulation of Shoot Growth in Greenhouse Peach

Yu Wang, Yonghong Li, Jie Li, Qihang Tian, Zhendong Tian, Ruifeng Chang, Guojian Liu, Zhaoyuan Wang*

Changli Institute of Pomology, Hebei Academy of Agriculture and Forestry Sciences, Qinhuangdao, Hebei, China

*Correspondence:
Zhaoyuan Wang
wy912963518@163.com

Abstract

Greenhouse high temperature and humidity induce excessive peach shoot growth, causing canopy closure, increased costs and poor fruit quality. Prohexadione-calcium (Pro-Ca) is a safe and effective plant growth retardant, but its molecular mechanisms regulating greenhouse peach growth have rarely been reported. Greenhouse-grown ‘Ruipan 25’ peach trees were treated with different Pro-Ca concentrations. We determined shoot growth and fruit quality, and performed hormone profiling, transcriptome sequencing and weighted gene co-expression network analysis (WGCNA) to explore Pro-Ca-responsive pathways and genes. The 400 mg/L Pro-Ca concentration optimally restrained shoot overgrowth, reduced leaf area, increased chlorophyll content, and improved fruit firmness and solid–acid ratio. Pro-Ca altered IAA, ZR and ABA levels, with GA_{34} and IAA-Asp as key metabolites. Pro-Ca regulation of shoot apices shows spatiotemporal specificity within 20 days after treatment: early responses involve

membrane signaling and hormone homeostasis maintenance, mid-term responses include cell wall remodeling and defense activation, and late-stage responses relate to growth recovery processes. Seven candidate genes such as *JAZ8* and *NAC37* were screened. This study demonstrated that Pro-Ca effectively inhibited excessive shoot growth in peach, a process accompanied by a series of biological responses. We identified key hormone metabolites and screened related candidate genes, providing a molecular basis and gene targets for further elucidating the mechanisms underlying growth regulation in fruit trees.

Keywords: Prohexadione-calcium; Peach; Vegetative shoot growth; Transcriptomics; WGCNA

Introduction

Peach (*Prunus persica* L. Batsch) belongs to the genus *Prunus* in the family Rosaceae. This ancient tree species is native to China, where it has been cultivated for over 3,000 years [1]. Consumers value peach fruits for their juiciness and palatable sweet-sour taste. Protected cultivation in plastic tunnels and solar greenhouses is an important approach to high-quality and efficient fruit production. By controlling temperature and humidity, this system prevents rain-induced quality loss associated with open-field cultivation and advances fruit maturation and market availability. However, the high temperature, high humidity, and low light intensity in protected environments promote excessive shoot growth, leading to canopy closure and reduced light penetration, thereby disrupting the balance between vegetative and reproductive growth and ultimately impairing fruit quality.

Methods commonly used to control overgrowth in protected cultivation include manual pinching, pruning, and plant growth regulator (PGR) application. PGRs regulate plant growth and development, with plant growth retardants having a key role in controlling shoot vigor [2]. In crop production, growth retardants reduce lodging risk in cereals such as rice exposed to

heavy rain and wind; in fruit trees, they promote a more compact canopy architecture, balance vegetative and reproductive growth, and improve fruit quality; in ornamental plants, they maintain compact growth and conserve greenhouse space[3]. Prohexadione-calcium (Pro-Ca), a gibberellin biosynthesis inhibitor, has several advantages over commonly used triazole compounds such as paclobutrazol (PBZ), including low residue levels, high crop safety, and limited suppression of root growth, and is widely used to manage excessive vegetative growth. Residues may remain after treatment with triazole-based plant growth regulators, such as paclobutrazol; repeated annual applications can cause a premature decline in tree vigor. Studies have also reported some mammalian toxicity for these chemicals [4]. Triazole-based regulators such as paclobutrazol inhibit the early steps of gibberellin biosynthesis, whereas Pro-Ca specifically blocks the 3β-hydroxylation process that converts GA_{20} to GA_1, thus reducing bioactive GA_1 accumulation [5]. In rice, Pro-Ca improves lodging resistance, and this effect is associated with increased culm wall thickness, lignin accumulation, and altered metabolism in basal internodes [6]. Furthermore, studies have shown that Pro-Ca suppresses vegetative growth in crops including corn seedlings[7], pear[8], apple[9-11], strawberry[12], and pepper [13]. Beyond regulating vegetative growth, reinforcing xylem structure and enhancing culm resistance, Pro-Ca also improves fruit quality in horticultural crops[14, 15].

Understanding of Pro-Ca-mediated growth regulation in peach remains limited, particularly under protected cultivation conditions. High temperature and humidity in greenhouses promote excessive vegetative shoot growth in peach trees, so safe and economical methods of growth regulation are urgently needed. Here, we examined the effects of Pro-Ca on shoot growth and fruit quality in protected-cultivated peach (*Prunus persica* L. cv. 'Ruipan 25') by applying four Pro-Ca concentrations during fruit development. We compared shoot vigor and fruit quality responses to different Pro-Ca concentrations, with the aim of identifying the optimal application concentration. We also combined transcriptomic profiling, endogenous

hormone measurements, and weighted gene co-expression network analysis (WGCNA) to identify key modules and candidate genes responsive to Pro-Ca treatment. These findings offer preliminary insights into the molecular mechanism by which Pro-Ca inhibits new shoot growth in protected-cultivated peach, and provide a theoretical basis for its popularization and application in peach cultivation.

Materials and methods

Test materials and treatment

The experiment was conducted from February to April 2024 in Greenhouse No.2 at the Changli Institute of Pomology, Hebei Academy of Agricultural and Forestry Sciences, Changli County, Qinhuangdao City, Hebei Province. Six-year-old peach trees of the cultivar ‘Ruipan 25’ were used as experimental materials. Trees sprayed with clean water served as the control (CK). Four concentrations of Pro-Ca, including 200 mg/L, 250 mg/L, 300 mg/L and 400 mg/L, were applied. Spraying was carried out three times at 20-day intervals on February 29, March 21 and April 9, with uniform application to the foliage until the leaf surfaces were just saturated to the point of dripping. Pro-Ca (15%, powder) was purchased from Zhengzhou Zhengshi Chemical Co., Ltd. (International Business Center, 72 Nongye Road, Zhengzhou, Henan Province, China). We adopted a randomized block design with three replicates per treatment and two trees per replicate, resulting in a total of six trees for each treatment. During sampling, shoot apices collected from the two trees within the same replicate were pooled into a single sample for hormone quantification and transcriptome sequencing. Shoot apex samples for hormone metabolite profiling and transcriptome analysis were harvested at 5, 10, 15 and 20 days after the first spray on February 29, and these samples only captured the early responses to the initial Pro-Ca application. Before the first spray, 10 current-year shoots were randomly tagged on the outer mid-canopy of each tree to measure their initial length. The length of the

tagged shoots was measured every five days after spraying to observe shoot growth performance.

Determination of shoot and leaf growth parameters

A measuring tape was used to measure shoots from the base to the apex every five days, and the increase in length was calculated. At 30 days after first spraying, functional leaves of comparable age and vigor (the 4th to 8th leaves from the shoot apex) were selected. The leaves were scanned, and leaf area was measured using image analysis software (LA-S, Wanshen, China), with 15 leaves assessed per treatment. Chlorophyll content was measured by acetone extraction with three replicates per treatment.

Measurement of fruit quality indices

Fruit quality indices were measured on the day of harvest, with 15 fruits assessed for each index. Individual fruits were weighed using an electronic balance. Fruit firmness was measured with a sclerometer. Soluble solids content (SSC) was determined using a refractometer (ATAGO PLA-1, Japan). Titratable acidity (TA) was measured with an automatic potentiometric titrator (ZD-2, Leici, Shanghai, China). The SSC-to-TA ratio was calculated as SSC divided by the corresponding TA value.

Quantification of hormone metabolites

For plant hormone quantification, shoot apices were collected from the control and 400 mg/L Pro-Ca treatment groups at four time points, immediately frozen in liquid nitrogen, and sent to Metware Biotechnology Co., Ltd. (Wuhan, China) (http://www.metware.cn/) for analysis. LC-MS/MS was used to quantify endogenous hormone metabolites in the samples. A tissue grinder was used to pulverize the frozen shoot apex samples at 30 Hz for 1 min. To 50 mg of ground sample, we added 10 μL of internal standard mixture (100 ng/mL) and 1 mL of methanol/water/formic acid extraction solution (15:4:1, v/v/v) and mixed thoroughly. After

vortexing for 10 min, samples were centrifuged at 12000 r/min for 5 min at 4 °C. The supernatant was collected in a new centrifuge tube and concentrated. After redissolution in 100 μL of 80% aqueous methanol, the residue was filtered through a 0.22 μm membrane, and the filtrate was placed in a sample vial for LC-MS/MS analysis. Liquid chromatography was performed as follows: compounds were separated on a Waters ACQUITY UPLC HSS T3 C18 column (1.8 μm, 100 mm × 2.1 mm i.d.). Ultra-pure water with 0.04% acetic acid served as Phase A, and acetonitrile with 0.04% acetic acid served as Phase B. Gradient elution followed this program: 0–1.0 min, 95% A / 5% B (V/V); 1.0–8.0 min, a linear change to 5% A / 95% B (V/V); 8.0–9.0 min, held at 5% A / 95% B (V/V); 9.1–12.0 min, returned to and held at 95% A / 5% B (V/V). The flow rate was 0.35 mL/min, the column was maintained at 40 ℃, and 2 μL was injected.

Mass spectrometry used the following settings: the electrospray ionization (ESI) source temperature was 550 °C, the mass spectrum voltage was 5500 V in positive ion mode and −4500 V in negative ion mode, and the curtain gas (CUR) pressure was 35 psi. Metabolites were identified by comparing mass spectrometry data with the Metware Database (MWDB) established using authentic standard compounds. Metabolite quantification was completed using the multiple reaction monitoring (MRM) on a triple quadrupole mass spectrometer. After mass spectrometry data were acquired for each sample, chromatographic peaks for all target metabolites were integrated, and metabolite amounts were calculated from the standard curves.

Transcriptome sequencing (RNA-seq)

Transcriptome sequencing was performed on control and 400mg/L Pro-Ca treatment samples collected at four time points. Metware Biotechnology Co., Ltd. conducted total RNA extraction and transcriptome sequencing. All extracted RNA samples were checked for quality. Poly(A) mRNA was enriched using Oligo(dT) magnetic beads and used to construct cDNA libraries that were subsequently assessed for quality. Libraries that passed quality checks were

sequenced on the Illumina platform, with three biological replicates per treatment. Raw sequencing reads were filtered to obtain clean data, and the clean reads were aligned to the reference genome using HISAT2 software. Read counts for each gene were obtained from the alignment results and genome annotations. Gene expression was measured using the FPKM (Fragments Per Kilobase of transcript per Million fragments mapped) metric. Differential expression between groups was analyzed using the DESeq2 software package. Genes with FDR < 0.05 and |log2 fold change| > 1 were classified as differentially expressed genes (DEGs).

Weighted gene co-expression network analysis (WGCNA)

Weighted gene co-expression network analysis (WGCNA) used online tools on the Metware Cloud Platform (https://cloud.metware.cn/) to examine co-expression patterns among functional genes. No additional expression filtering was applied to the input genes. The module merge cut height was set to 0.25, and the minimum module size was 50. Cytoscape_v3.10.4 software was used to visualize gene interaction networks.

qPCR validation

All gene-specific primers were designed using Primer Premier 5.0 software, and their specificity was verified via NCBI Primer-BLAST. All primers were synthesized by Sangon Biotech (Shanghai) Co., Ltd. The β-actin gene was used as a reference gene for expression normalization. Reverse transcription was performed using the Evo M-MLV RT Mix Kit with gDNA Clean for qPCR Ver.2 (Code No. AG11728, Accurate Biology). Quantitative real-time PCR was carried out with 2× SG Green qPCR Mix (AG11701, Accurate Biology) on a Bio-Rad CFX Manager real-time PCR system. Three biological replicates were used for each group, and each sample was assayed in three technical replicates. The relative gene expression levels were calculated using the $2^{-\Delta\Delta Ct}$ method.

Statistical analysis

Physiological indices were analyzed by one-way analysis of variance (ANOVA) in IBM SPSS Statistics 26.0. Differences were assessed using Duncan's multiple range test with significance set at $p < 0.05$. Figures showing physiological indices were generated using GraphPad Prism 9.

Results

Effects of Pro-Ca on shoot growth increment and leaf traits

We measured the shoot growth increment for each treatment and the control group every five days. All Pro-Ca treatments had markedly lower shoot growth increments than the water control before April 1. After April 1, shoot growth fluctuated markedly in the 250 mg/L and 300 mg/L treatments, indicating inconsistent inhibition at medium and low Pro-Ca concentrations. Across the measurement period, the 400 mg/L treatment consistently maintained a lower shoot growth increment than the control and most effectively inhibited new shoot elongation (Fig.1A).

Measurements of peach leaves exposed to different Pro-Ca concentrations showed that foliar Pro-Ca application significantly reduced leaf area and increased chlorophyll a, chlorophyll b, and total chlorophyll (a+b) contents (Fig.1B, C, D, E). Relative to the control group, chlorophyll a, chlorophyll b, and total chlorophyll contents increased by 21.8%, 43.0%, and 26.4%, respectively, under the 400 mg/L treatment. These results show that Pro-Ca increases leaf photosynthetic pigment levels, which may promote leaf photosynthetic capacity.

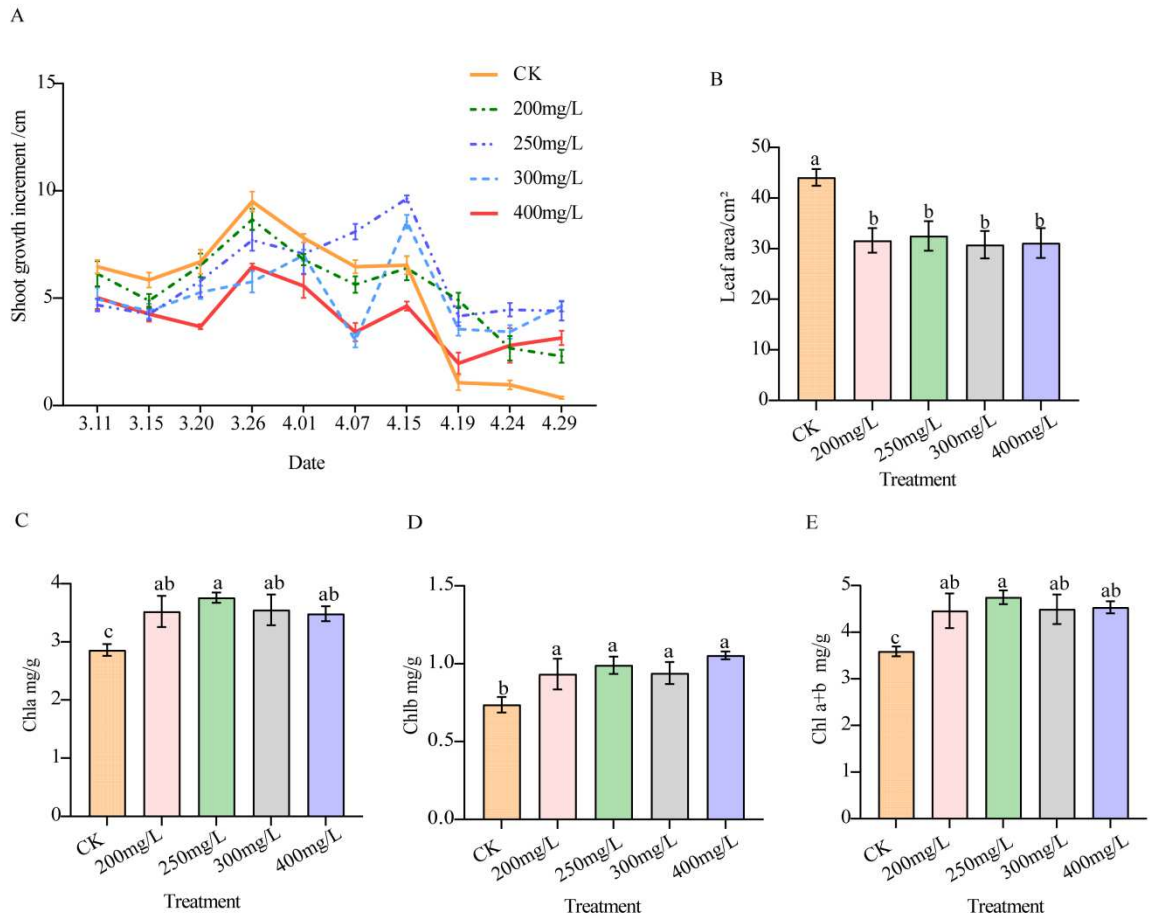

Fig.1 Shoot growth and leaf characteristics of peach trees under protected cultivation following application of different Pro-Ca concentrations. **A** Increment in shoot growth, values represent means ± SE (n = 10). **B** Leaf area, values represent means ± SE (n = 15). **C** Chla; **D** Chlb; **E** Chl(a+b), values represent means ± SE (n = 3). Different letters above the bars denote significant differences ($p < 0.05$) as determined by Duncan's multiple range test.

Effects of Pro-Ca on fruit quality

Fruit quality indices were measured to assess whether foliar Pro-Ca application adversely affects peach fruit quality. Relative to the control, the effect of Pro-Ca on fruit weight exhibited no regular concentration-dependent trend (Fig. 2A). Fruit weight was significantly increased under 200 mg/L and 300 mg/L Pro-Ca treatments, whereas no significant differences were observed at 250 mg/L and 400 mg/L compared with the control. All Pro-Ca treatments significantly increased fruit firmness, which may contribute to improved postharvest storage

performance (Fig. 2B). The 200, 250 and 300 mg/L Pro-Ca treatments significantly increased fruit soluble solids content (SSC) (Fig. 2C). The 400 mg/L treatment significantly reduced titratable acid content (TA) by 11.29% and increased the SSC-TA ratio by 14.51% (Fig. 2D, E). These results indicate that foliar Pro-Ca application positively modulates multiple peach fruit quality traits in a concentration-specific manner.

In terms of shoot growth inhibition, 400 mg/L Pro-Ca showed the strongest suppressive effect. Meanwhile, this concentration uniquely reduced fruit titratable acid and improved the SSC-TA ratio. Therefore, the 400 mg/L treatment and the control were selected for combined transcriptome and hormone metabolome analysis.

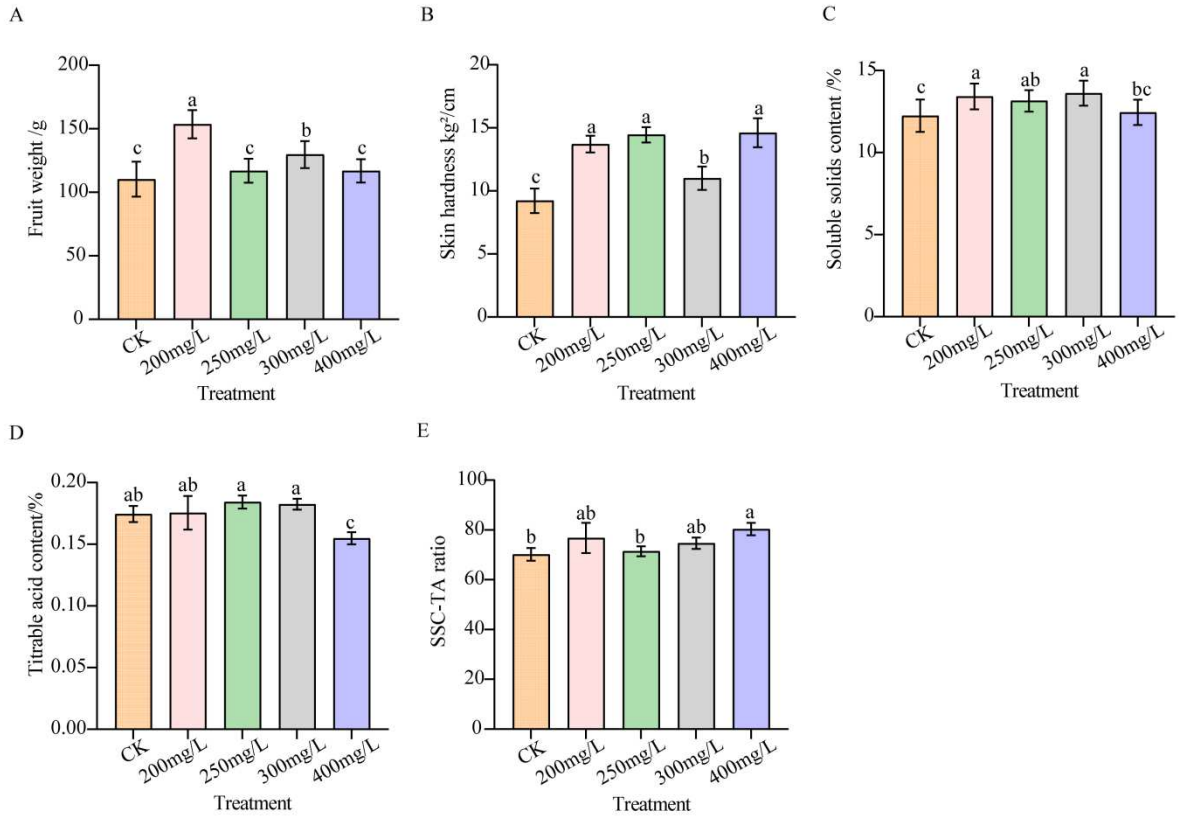

Fig.2 Fruit quality following application of different Pro-Ca concentrations. Values represent means ± SE (n = 15). Different letters above the bars denote significant differences ($p < 0.05$) as determined by Duncan's multiple range test.

Analysis of hormone metabolites in shoot apices at different time points

Targeted hormone metabolite profiling was conducted to compare the control and 400mg/L Pro-Ca treatment groups at four time points (5, 10, 15, and 20 d). In total, 35 hormone metabolites were identified, including auxins, abscisic acid, cytokinins, gibberellins, and strigolactones. Screening with thresholds of $|\log_2 FC| > 1$ and FDR < 0.05 identified 23 differential hormone metabolites. Venn diagrams were used to compare differential hormones between the Pro-Ca treatment and control groups at the four time points (Fig.3A). The greatest number of differential hormones (12) was detected at 5 d after treatment, followed by 8, 11, and 10 at the subsequent three time points, suggesting that peach shoots showed the strongest hormonal response to Pro-Ca early after treatment. Two hormones differed significantly at all four time points, namely GA_{34} (gibberellin 34) and IAA-Asp (indole-3-acetic acid-aspartate). At all four sampling time points after Pro-Ca treatment, GA_{34} levels were consistently lower, while IAA-Asp levels were consistently higher. These two metabolites may have key roles in Pro-Ca-mediated regulation of new shoot growth in peach.

A heatmap was used to show the accumulation patterns of hormone metabolites that differed significantly between groups (Fig.3B). GA_{19}, GA_{34}, GA_8, and IAA-Leu levels were significantly lower in the Pro-Ca treatment group, whereas GA_{20}, GA_{15}, and IAA-Asp levels were significantly higher. BAP, GA_7, and cZROG increased significantly at 5 d, 15 d, and 20 d after Pro-Ca treatment, respectively. ABA-ald levels were significantly elevated from 10 d to 15 d, while 2MeScZ and GA_{53} levels were significantly reduced at 20 d.

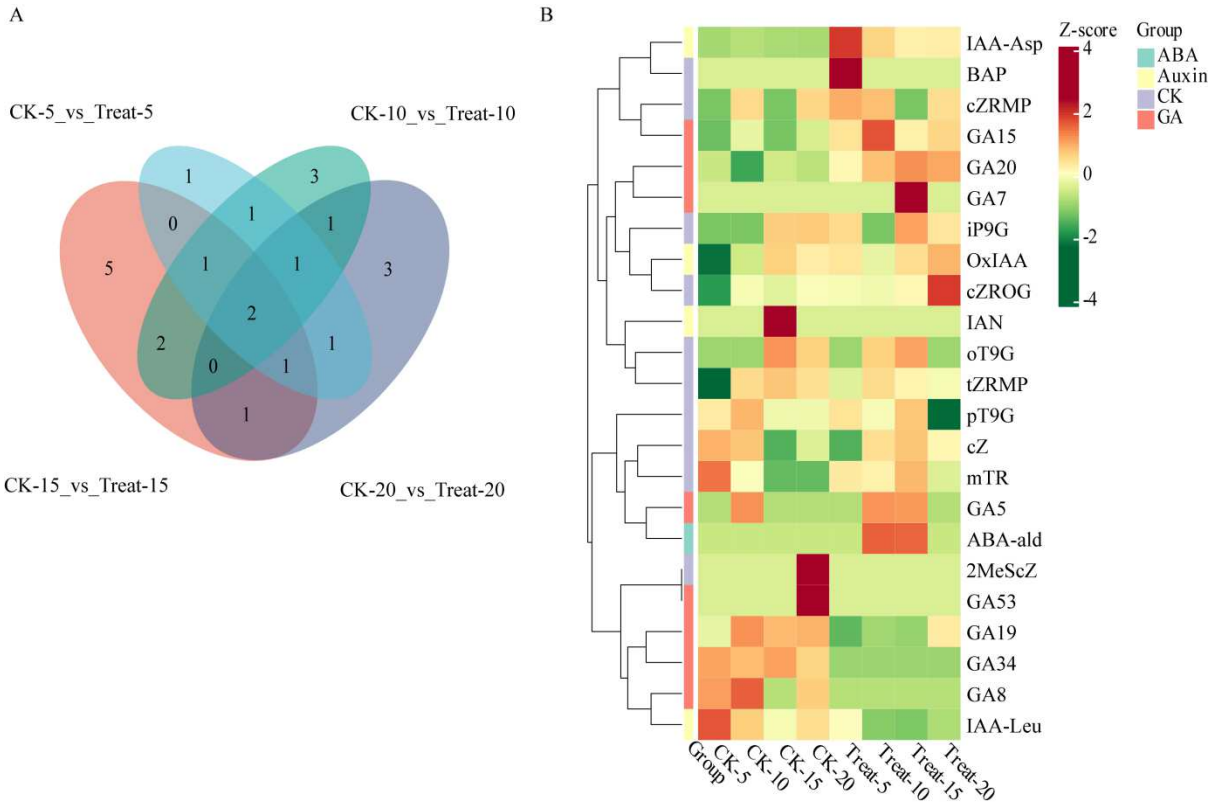

234

235 **Fig. 3** Analysis of hormone metabolites. **A** Venn diagram showing differential hormone

236 metabolites across time points. **B** Heatmap showing the contents of differential metabolites.

237 **Transcriptome analysis of shoot apices at different time points**

238 ***DEGs at different time points***

239 To examine temporal changes in differentially expressed genes (DEGs) in response to Pro-Ca,

240 shoot apices from the control (CK) and 400 mg/L Pro-Ca treatment (Treat) groups were

241 sequenced at four time points. Correlations in gene expression between samples were assessed

242 by calculating pearson correlation coefficients across all genes for each sample pair and

243 displaying them as heatmaps (Fig. 4A). Biological replicates were highly correlated in all

244 groups, supporting the reproducibility of the gene expression data. Principal component

245 analysis (PCA) showed that PC1 and PC2 explained 36.84% and 23.3% of the total variance,

246 respectively (Fig. 4B). Samples separated clearly according to Pro-Ca treatment and sampling

247 time, indicating that both treatment and sampling time strongly influenced the peach shoot tip
248 transcriptome.

249 Using the criteria $|\log_2 FC| > 1$ and FDR < 0.05, 2466 significant DEGs were identified
250 across four comparisons, namely CK-5_vs_Treat-5, CK-10_vs_Treat-10, CK-15_vs_Treat-15,
251 and CK-20_vs_Treat-20. Their overlap was examined using a Venn diagram (Fig. 4C). The
252 largest number of DEGs (1699) occurred in CK-20_vs_Treat-20, followed by
253 CK-5_vs_Treat-5 (660), CK-10_vs_Treat-10 (307), and CK-15_vs_Treat-15 (296). Seven
254 DEGs were shared across all four time points, including *Prupe.3G131500* (*bHLH36*),
255 *Prupe.2G272500* (*ERF106*), *Prupe.3G144500* (*TRPA2*), *Prupe.4G082500* (*JAZ8*),
256 *Prupe.6G249300* (*ZAT11*), *Prupe.6G138700* (*BDH*), and *Prupe.2G129400* (*ERF2*).

257 Up-regulated and down-regulated DEGs were counted for each comparison group (Fig.
258 4D). There were 477 up-regulated and 183 down-regulated DEGs at 5 d, 83 up-regulated and
259 224 down-regulated DEGs at 10 d, 155 up-regulated and 141 down-regulated DEGs at 15 d,
260 and 933 up-regulated and 766 down-regulated DEGs at 20 d. The early transcriptional response
261 to Pro-Ca (5 d) was thus dominated by gene up-regulation. At the middle stage (10 d), down-
262 regulated genes became more numerous, indicating that transcriptional inhibition
263 predominated. The numbers of up-regulated and down-regulated genes were similar at 15 d.
264 By 20 d, numerous DEGs were detected again, and up-regulated genes exceeded down-
265 regulated genes.

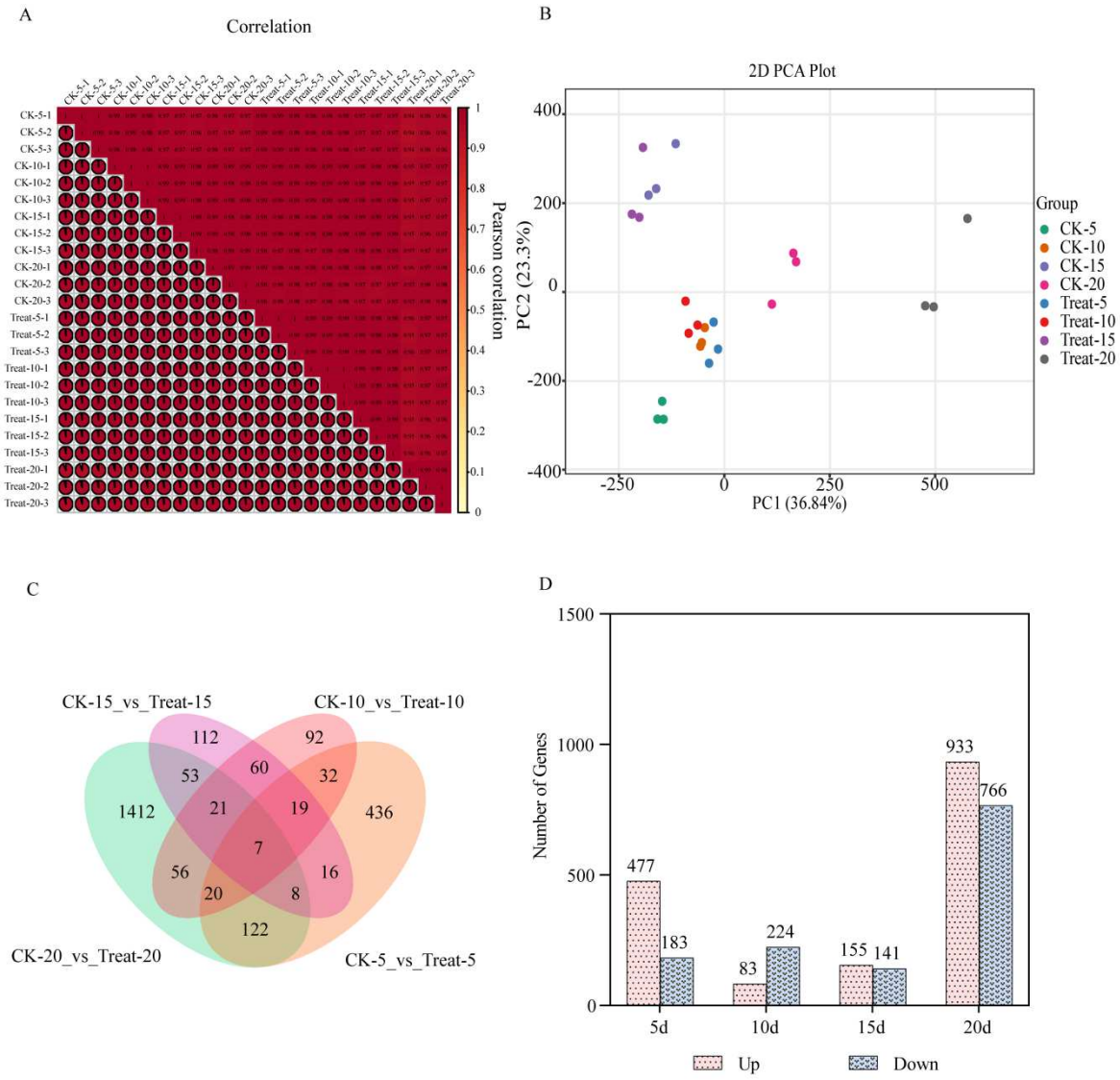

Fig.4 DEGs analyzed across sampling time points. **A** Pearson correlations between sample gene expression profiles. **B** Sample distribution in principal component analysis. **C** Venn diagram showing differential genes across time points. **D** Counts of up-regulated and down-regulated DEGs at each time point.

KEGG pathway enrichment analysis of DEGs

KEGG enrichment analysis was conducted for DEGs from four comparisons at each sampling time point[16-19]. Terms containing < 3 genes were excluded, and the top 10 enriched pathways at each time point were ranked and displayed by adjusted P-values (Padj), with color intensity indicating Padj and bubble size indicating gene number (Fig. 5). The biosynthesis of

secondary metabolites pathway was significantly enriched at every time point, suggesting that Pro-Ca-mediated regulation of shoot growth is closely associated with the biological processes of secondary metabolites (including terpenoids, flavonoids, and anthocyanins). At 5 d, the main enriched pathways were sesquiterpenoid and triterpenoid biosynthesis, stilbenoid, diarylheptanoid and gingerol biosynthesis, and ABC transporters. At 10 d, plant-pathogen interaction and MAPK signaling pathway (plant) were significantly enriched, suggesting enhanced stress tolerance in shoots. At 15 d, enrichment was prominent in secondary metabolite biosynthesis and phenylpropanoid biosynthesis pathways. At 20 d, more pathways were significantly enriched, and biosynthesis of secondary metabolites contained the most DEGs. DNA replication, anthocyanin biosynthesis, plant hormone signal transduction, and MAPK signaling pathway were also significantly enriched at this stage.

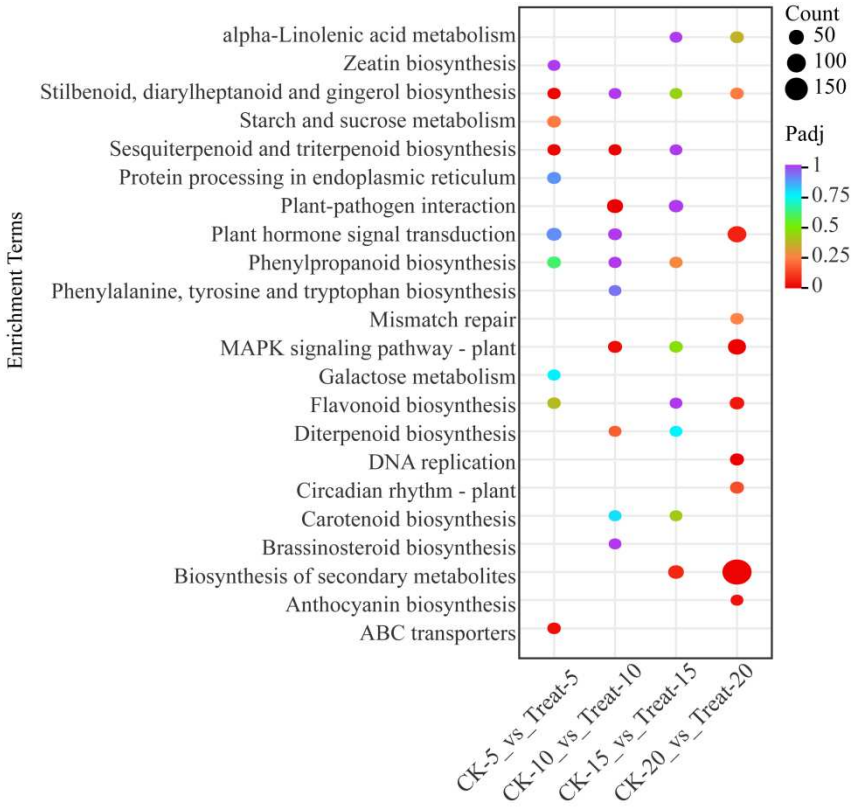

Fig.5 KEGG pathway analyses of DEGs comparing the Pro-Ca treatment with the control at 5 d, 10 d, 15 d, and 20 d.

290 ***GO enrichment analysis of DEGs***

291 GO enrichment analyses of DEGs at the four time points used an adjusted P-value threshold <
292 0.05, and the top 20 enriched terms per time point were displayed (Fig. 6). At 5 d, enriched
293 biological process terms mainly concerned regulation of signal transduction and cell
294 communication, together with metabolic pathways involving terpenoids, jasmonic acid, auxin,
295 and chlorophyll. In the cellular component category of GO annotation, DEGs were mainly
296 enriched in the plasma membrane and its anchored components, indicating that these DEGs
297 function mainly at the plasma membrane. For molecular function, UDP-glycosyltransferase
298 activity showed the strongest enrichment. At 10 d, the main enriched biological process terms
299 concerned isoprenoid biosynthesis, auxin biosynthesis, and glucan metabolic processes,
300 together with defense response regulation and oxidative stress response. Molecular function
301 terms included tetrapyrrole binding, monooxygenase activity, lyase activity, and xyloglucan
302 transferase activity. At 15 d post-treatment, significant enrichment of biological process terms
303 centered on cell wall-related processes, including response to wounding, cellular glucan
304 metabolic process, cell wall polysaccharide metabolic process, hemicellulose metabolic
305 process, lignin biosynthetic process, and plant-type secondary cell wall biogenesis.
306 Gibberellin-associated biological-process terms were also enriched, including diterpenoid
307 biosynthetic process and negative regulation of GA-mediated signaling pathways, as was the
308 ethylene-activated signaling pathway. Enriched molecular function terms included gibberellin
309 2-beta-dioxygenase activity and two transferase activities related to cell-wall modification:
310 xyloglucan:xyloglucosyl transferase activity and glucosyltransferase activity. Cellular
311 component terms primarily concerned the apoplast, suggesting that this was the main functional
312 site at this stage. At 20 d post-treatment, enriched biological process terms spanned several
313 functional categories. Terms concerning DNA homeostasis included cellular response to DNA
314 damage stimulus, DNA-templated DNA replication, double-strand break repair and DNA

integrity checkpoint signaling. Significant enrichment was also found for the abscisic acid-activated signaling pathway, response to oxidative stress, cell-cycle-phase transition and its negative regulation, and flavonoid biosynthetic process. Enriched cellular component terms included nuclear chromosome, MCM complex and DNA polymerase complex. Molecular function terms included monooxygenase activity, abscisic acid binding, DNA helicase activity, and cell-wall-related xyloglucosyl transferase activity.

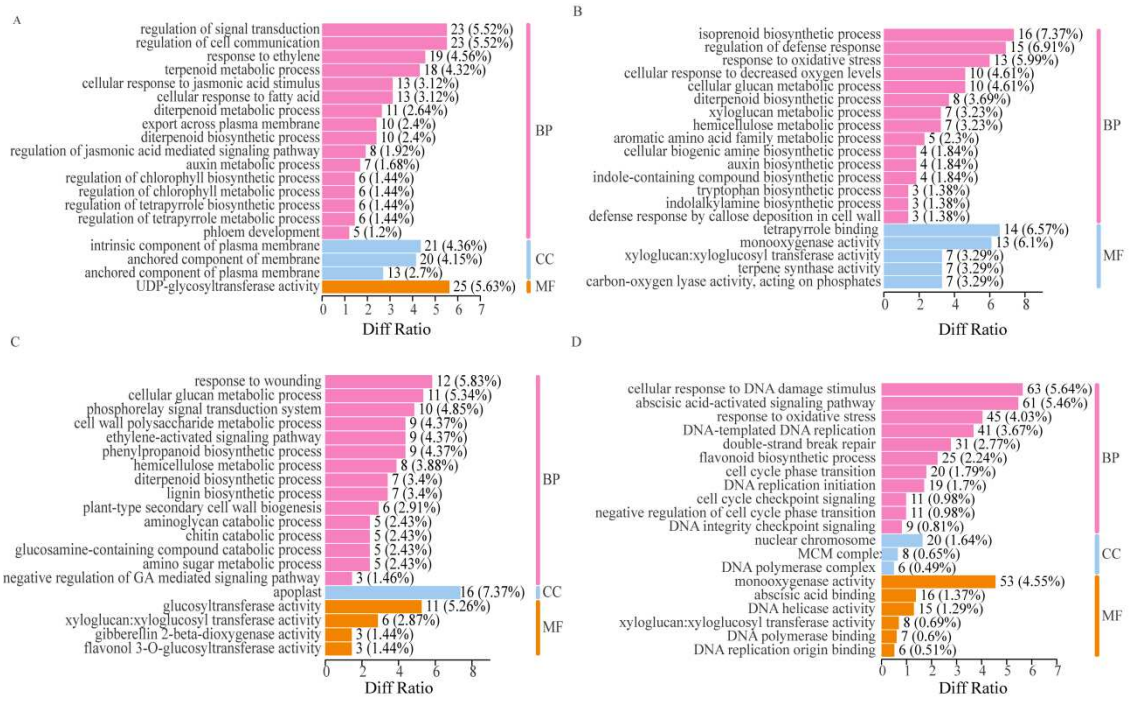

Fig.6 GO terms enriched among DEGs comparing the Pro-Ca treatment with the control at 5 d, 10 d, 15 d, and 20 d.

Integrated WGCNA analysis based on transcriptomes and phytohormone metabolomes

WGCNA was then applied to 2466 DEGs and 35 targeted hormone metabolites. Genes were clustered by their expression profiles, and those with similar patterns were assigned to co-expression modules distinguished by color. We selected the soft-thresholding power using the pickSoftThreshold function to satisfy the scale-free topology criteria. The scale-free topology fit index (signed R^2) and mean connectivity under each tested power were calculated

and visualized(Fig. S1). We selected a soft-threshold power of 20, which was the minimum value that made the signed R^2 exceed 0.8. This analysis identified 11 co-expression modules. With thresholds of $|r| \geqslant 0.8$ for the correlation coefficient and $p < 0.05$, two core modules (magenta and yellow) were strongly correlated with hormone-metabolism signatures, suggesting their involvement in Pro-Ca-mediated regulation of peach shoot growth (Fig. 7C). Gene expression patterns within each module across treatment time-points are shown in the corresponding figure (Fig. 7D, E). Yellow module gene expression was clearly suppressed at 5 d in the treatment group. In the control group, magenta module genes had low expression before activation at 15 d, and expression remained high from 15 d to 20 d. In the treatment group, magenta-module expression was slightly higher than in the control at 5 d; however, activation and high expression occurred at 20 d, a 5-day delay relative to the control.

Genes in each co-expression module were annotated using GO, and enriched terms containing < 3 genes were excluded. The top 10 enriched terms with adjusted P-value < 0.05 were displayed. Magenta module genes were significantly enriched in plant cell-wall-related biological processes, including phenylpropanoid biosynthetic process and lignin biosynthetic process, with 12 genes identified from this module (Fig. 8A). A co-expression network included all 84 genes in the magenta module, with color intensity representing gene connectivity within the module. Within this network, we examined the 12 candidate genes associated with cell-wall metabolism, phenylpropanoid biosynthesis and lignin biosynthesis pathways. *FLA11* (*Prupe.6G238300*), *NAC37* (*Prupe.7G166300*) and *RIC4* (*Prupe.6G360900*) had high connectivity within this subset, which can serve as priority candidates for further dissection of the regulatory mechanism underlying these pathways (Fig. 8C).

Functional annotation of the yellow module identified four pathways related to hormone metabolism, including terpene synthase activity, diterpenoid biosynthetic process, regulation of jasmonic acid mediated signaling pathway, and auxin biosynthetic process (Fig. 8B).

Homology-based sequence alignment of genes in these pathways identified four candidates associated with hormone-mediated shoot growth: *JAZ10* (*Prupe.1G218500*), *JAZ8* (*Prupe.4G082500*), *JOX2* (*Prupe.2G250900*), and *TRPA1* (*Prupe.3G144300*). The network visualization include all genes in the module and is presented in the figure (Fig. 8D).

Using the gene annotations (Table 1), we examined temporal expression patterns of the seven core candidate genes in the Yellow and Magenta modules (Fig. 8E). In the Yellow module, the jasmonic acid pathway genes *JAZ8*, *JAZ10*, and *JOX2*, together with *TRPA1* involved in tryptophan synthesis for auxin biosynthesis, showed high expression in the control at the early stage (5 d), but lower expression after Pro-Ca treatment. *JAZ8* and *JAZ10* were downregulated at all four time points, and *TRPA1* expression was significantly reduced at the later stage (20 d). In the Magenta module, expression of the cell wall-related genes *FLA11*, *RIC4*, and transcription factor gene *NAC37* was higher in the Pro-Ca treatment group than in the control at the early stage (5 d), whereas *FLA11* and *NAC37* expression was significantly lower between 10 and 15 d.

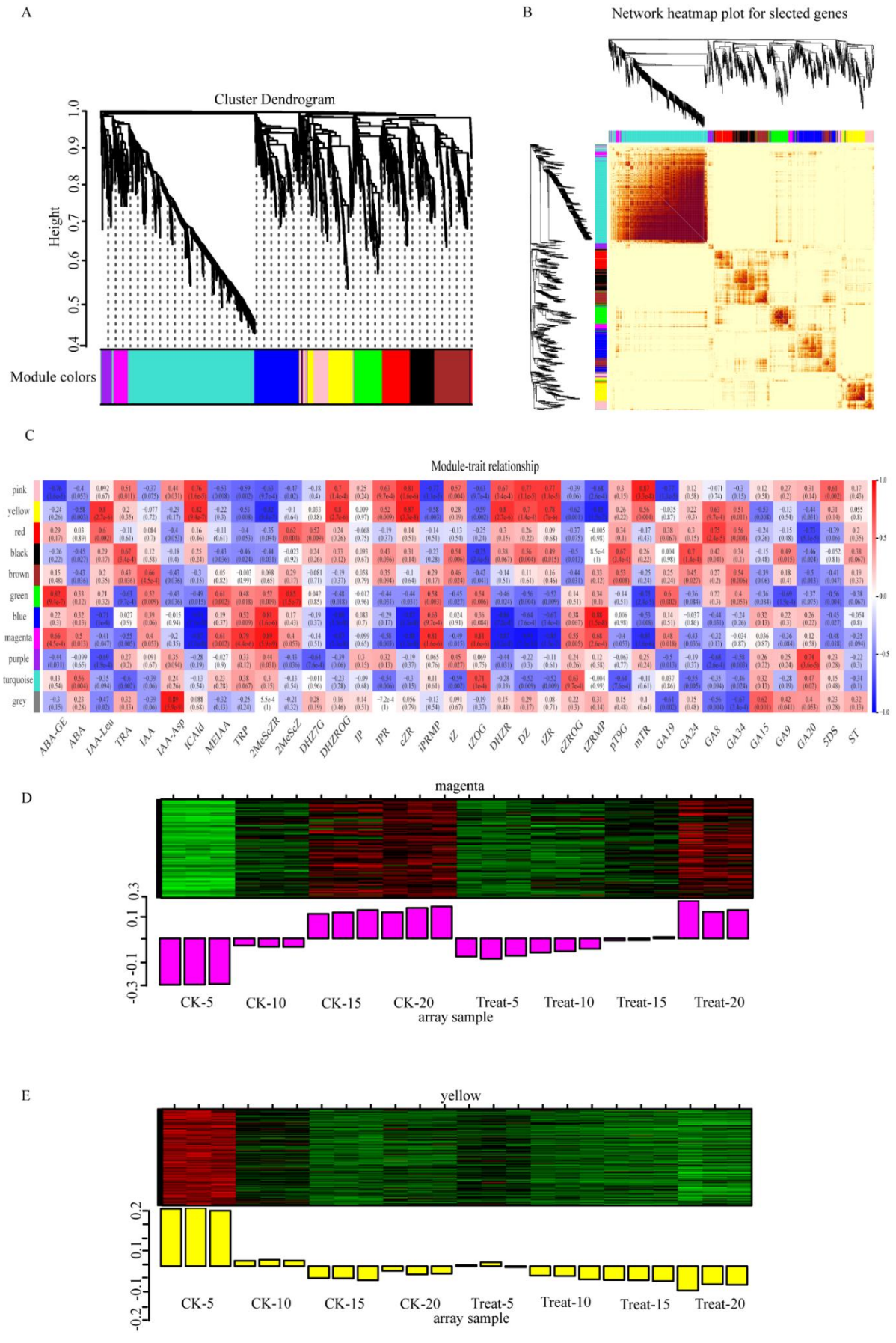
A
Cluster Dendrogram
Height
Module colors
B
Network heatmap plot for slected genes
C
Module-trait relationship
pink
yellow
red
black
brown
green
blue
magenta
purple
turquoise
grey
ABA-GE
ABA
IAA-Leu
TRA
IAA
IAA-Asp
ICAld
MEIAA
TRP
2MeSeZR
2MeSeZ
DHZ7G
DHZROG
IP
IPR
cZR
iPRMP
tZ
tZOG
DHZR
DZ
tZR
cZROG
tZRMP
pT9G
mTR
GA19
GA24
GA8
GA34
GA15
GA9
GA20
5DS
ST
D
magenta
CK-5
CK-10
CK-15
CK-20
Treat-5
Treat-10
Treat-15
Treat-20
array sample
E
yellow
CK-5
CK-10
CK-15
CK-20
Treat-5
Treat-10
Treat-15
Treat-20
array sample

369

Fig.7 WGCNA identification of key modules and hub genes associated with peach shoot growth following Pro-Ca treatment. (A) Hierarchical clustering tree showing modules of co-expressed genes in peach shoots treated with Pro-Ca. (B) Network heatmap for selected genes. (C) Heat map showing module–trait relationships. Each cell gives the correlation coefficient (upper) and p-values (lower in parentheses) for the module-trait association. (D, E) Expression patterns for genes in the magenta and yellow modules. The upper panel presents a clustered heatmap of gene expression within each module, where red indicates high expression and green indicates low expression. The lower panel shows the module eigengene expression pattern across samples.

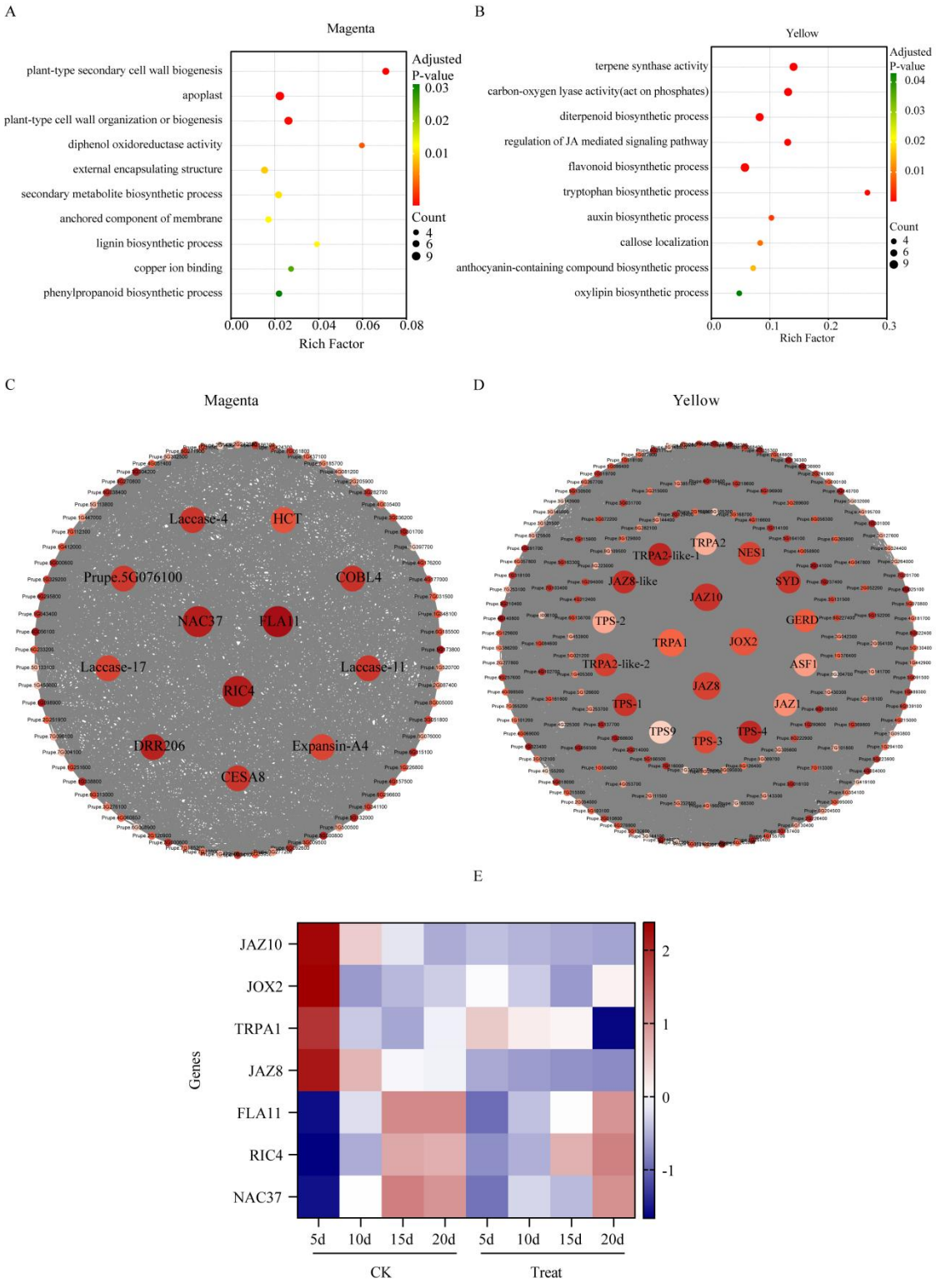

Fig.8 Functional enrichment and co-expression networks of key modules in Pro-Ca-treated peach shoots. (A) GO enrichment of genes assigned to the magenta module. (B) GO enrichment of genes assigned to the yellow module. (C,D) Co-expression networks for magenta and yellow module genes. Larger nodes represent hub genes. (E) Heatmap showing hub gene expression

384 in the magenta and yellow modules. FPKM values were normalized by Z-scores; red indicates
385 high expression and blue indicates low expression.

386 **qRT-PCR validation**

387 To verify the reliability of transcriptome sequencing data, seven genes screened from the
388 MEmagenta and MEyellow modules were subjected to qRT-PCR validation. The expression
389 trends of these seven genes across different treatment stages (Figure 9) were highly consistent
390 with the transcriptome data (Figure 8E). For example, *JAZ10* and *JAZ8* exhibited a time-
391 dependent gradual reduction in expression under control conditions and were persistently
392 downregulated in the treatment group, while RIC4 expression displayed a steadily rising trend
393 in both control and treatment groups. This consistency in expression trends confirms the
394 stability and accuracy of the transcriptome data and supports the reliability of the modules and
395 hub genes identified by WGCNA.

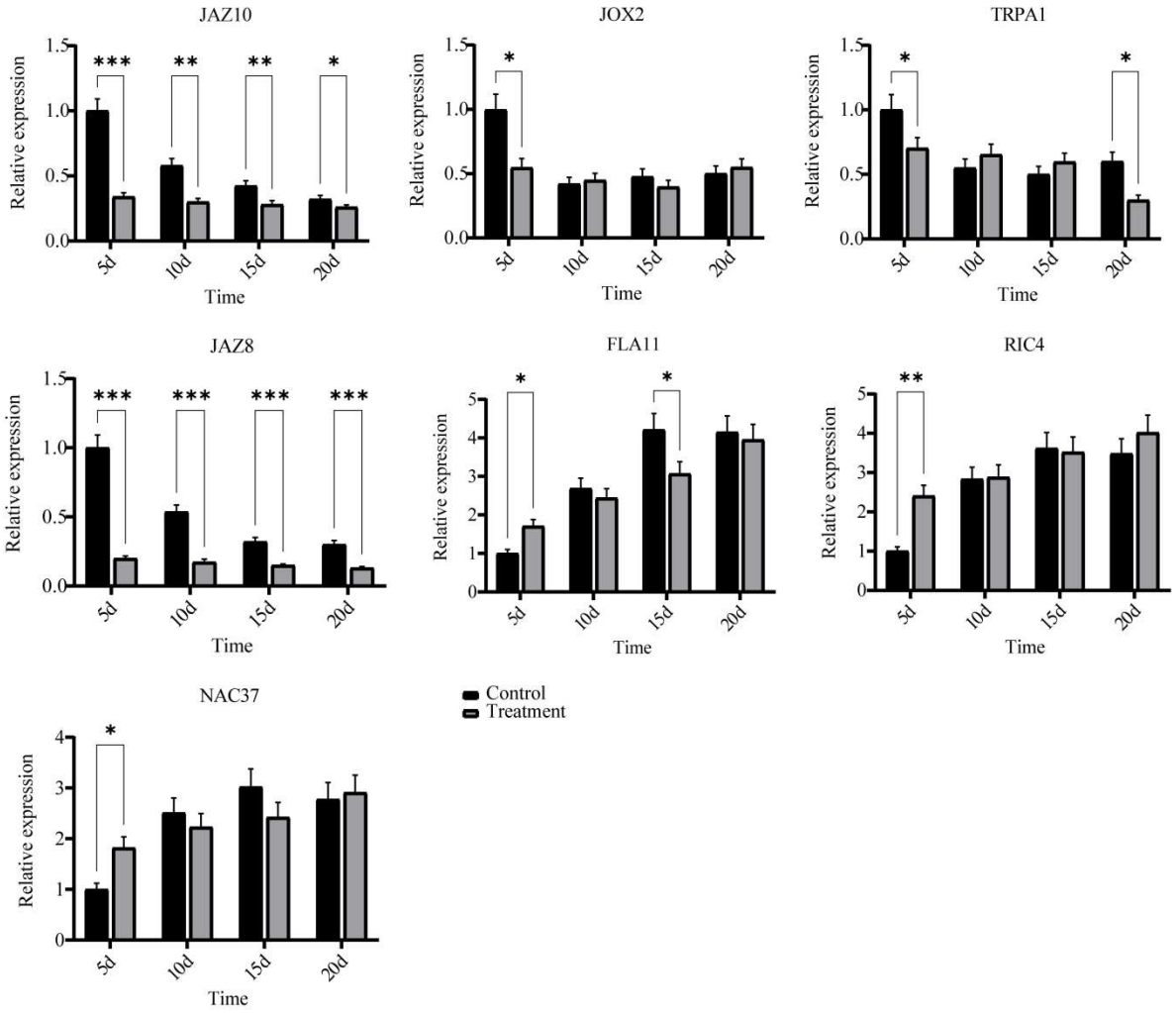

Fig.9 qRT-PCR validation results of seven hub genes at different treatment stages. The relative expression levels were calculated by the ($2^{-\Delta\Delta CT}$) method, with error bars representing the standard error. Black bars indicate the control group, and gray bars indicate the treatment group. The x-axis represents treatment time, and the y-axis represents gene expression. *, $p < 0.05$; **, $p < 0.01$; ***, $p < 0.001$.

Discussion

Regulation of vegetative growth and concomitant effects on fruit quality by Prohexadione-calcium in greenhouse-grown peach

Prohexadione-calcium (Pro-Ca), a gibberellin synthesis inhibitor, is widely used in agriculture to regulate crop growth and limit vegetative vigor. Peach trees exhibit vigorous bud burst and branching, and high-temperature and high-humidity conditions in greenhouses often promote excessive shoot elongation, creating a demand for safe and efficient plant growth regulators to control shoot growth and reduce labor for pinching and pruning. Our results showed that Pro-Ca markly reduced shoot growth and leaf area in greenhouse-grown peach, while significantly increasing leaf chlorophyll a and chlorophyll b contents. These results agree with earlier studies showing that foliar Pro-Ca application can inhibit shoot elongation and leaf expansion, increase leaf chlorophyll content, and improve canopy light penetration and ventilation in fruit trees[2, 20-22]; molecular analyses also revealed that Pro-Ca altered the expression of genes related to photosynthesis (*PsbS*, *PsbD*) and chlorophyll metabolism (*PPD*)[23]. In this study, shoot growth dynamics under the low-concentration treatment (200 mg/L) resembled those of the control, indicating limited inhibition. Moderate concentrations (250 and 300 mg/L) produced unstable inhibitory effects on shoot growth, whereas the 400 mg/L treatment exerted the strongest inhibition. Shoot growth increased rapidly at the later stage of observation. This rebound may reflect the gradual metabolic turnover of Pro-Ca within plants. As the inhibitory activity of Pro-Ca diminishes over time, accumulated GA precursors can be converted into bioactive GAs, leading to late-season shoot regrowth [20, 23].

Vegetative growth and reproductive development in fruit trees follow a source–sink relationship, and previous studies have shown that Pro-Ca promotes the transfer of non-structural carbohydrates from source to sink organs [24]. The present study revealed that Pro-Ca did not induce consistent reductions in fruit weight across the tested concentrations, which has important implications for practical field application. The beneficial effect of Pro-Ca on fruit hardness may be related to previous observations that Pro-Ca increases the cell-wall

thickness of parenchyma tissues[25]. Our data also showed that low to moderate concentrations (200–300 mg/L) significantly increased soluble solids content, whereas 400 mg/L significantly reduced titratable acidity, producing a markedly higher soluble solids-to-titratable acidity ratio. Together, these results indicate that an appropriate Pro-Ca concentration effectively controls shoot growth and can improve peach fruit flavor and storage quality to some extent. Similar improvements in fruit quality following Pro-Ca treatment have also been reported in grape [14]and guava[15].

Prohexadione-calcium mediates endogenous hormone homeostasis in shoot apices to regulate shoot growth

Pro-Ca inhibits gibberellin biosynthesis at a downstream step [26]. In this study, GA_{20} levels were higher in the treatment group than in the control at all four time points, consistent with the proposed model that Pro-Ca inhibits 3β-hydroxylation of GA_{20} to GA_1. Comparison of hormone metabolites between treatment and control groups across the four time points showed the most differential hormones at 5 d post-treatment, indicating that the endogenous hormonal response to Pro-Ca in shoot apices was strongest at the early stage. GA_{34} is an inactive catabolite formed through GA2-oxidase-mediated degradation of bioactive gibberellins (GAs)[27-30]. Experiments have shown significantly elevated GA_{34} levels in *GA2ox*-overexpressing dwarf lines [31], linking GA_{34} accumulation to dwarf phenotypes, a phenomenon attributable to accelerated catabolism of bioactive GAs by *GA2ox* overexpression, leading to substantial GA_{34} accumulation. Pro-Ca treatment in this study inhibited shoot growth while concomitantly decreasing GA_{34} content. This is because Pro-Ca inhibits the biosynthesis of bioactive GAs, lowering the levels of bioactive GAs available for GA2ox-mediated degradation and consequently reducing the content of their catabolite GA_{34}. IAA-Asp is an auxin-amino acid conjugate produced by GRETCHEN HAGEN 3 (GH3) enzymes, which inactivate free active IAA and regulate its homeostasis. Higher IAA-Asp levels generally

indicate a smaller pool of bioavailable free IAA, and hence inhibition of cell elongation [32]. In our study, GA_{34} and IAA-Asp differed significantly between groups at all four time points, with consistently lower GA_{34} and higher IAA-Asp levels. These metabolites serve as key hormonal markers strongly associated with shoot growth status and reflect dynamic changes in endogenous hormone metabolism accompanying Pro-Ca-triggered shoot growth inhibition in peach. Beyond these two hormones with consistent differences across time points, several gibberellin intermediates, auxin derivatives, cytokinins, and abscisic acid components showed time-specific increases or decreases. For example, GA_{19}, GA_8, and IAA-Leu levels decreased, while GA_{20} and GA_{15} levels increased; GA_7, GA_{53}, and CTK- and ABA-related components also varied over time. These results indicate that Pro-Ca affects gibberellin biosynthesis as well as several other hormone metabolic pathways, including auxin, cytokinin, and abscisic acid, which together contribute to shoot growth suppression. This agrees with earlier observations in sweet cherry [33], where Pro-Ca caused temporal changes in several endogenous hormones, including IAA, ZR, and ABA, and these hormone metabolites jointly respond to Pro-Ca-mediated regulation of shoot growth.

Transcriptomic and WGCNA analyses reveal candidate genes for Prohexadione-calcium -regulated peach shoot growth

Prohexadione-calcium is a gibberellin inhibitor widely used in agriculture. Beyond its established role in suppressing gibberellin biosynthesis, evidence indicates that Pro-Ca also influences endogenous hormone cross-talk, secondary metabolism, and stress tolerance in plants[34-36]. In this study, transcriptome sequencing and WGCNA were used to examine dynamic transcriptional changes associated with Pro-Ca-regulated shoot growth. The response of greenhouse-grown peach to Pro-Ca showed pronounced spatiotemporal patterns. Alongside suppression of the gibberellin pathway, Pro-Ca sequentially affected biological processes involving membrane signal perception, homeostatic regulation of auxin and jasmonic acid, cell

480 wall remodeling, and defense-related pathways, followed by recovery-associated processes
481 such as DNA replication at later stages, as the chemical effect weakened over time.

482 At 5 d post-treatment, upregulated DEGs were more numerous than downregulated DEGs.
483 KEGG analysis showed significant enrichment of sesquiterpenoid and triterpenoid
484 biosynthesis, stilbenoid-related secondary metabolism, and ABC transporter pathways.
485 Enriched terms included signal transduction, cell communication, auxin metabolism, and
486 terpenoid metabolism, together with GO terms for chlorophyll metabolism, consistent with the
487 changes in chlorophyll content measured in this study.

488 Jasmonic acid (JA) is a phytohormone involved in defense responses and the regulation
489 of plant growth. It inhibits plant growth and interacts antagonistically with gibberellin [37, 38],
490 and auxin [39]. JA and GA engage in canonical signaling cross-talk, in which JA suppresses
491 GA-mediated vegetative growth through the COI1-JAZ-DELLA-PIF module to balance
492 growth and defense [37]. Therefore, the JA signaling pathway acts as a central hub in regulating
493 the defense–growth antagonism. Previous studies have shown that exogenous JA application
494 or overexpression of JA-responsive transcription factors can inhibit plant growth [40]. JAZ8
495 and JAZ10 proteins act as repressors of JA signaling and suppress the activity of multiple JA-
496 responsive transcription factors[41, 42]. *TRPA1* encodes the alpha subunit of tryptophan
497 synthase and participates in tryptophan biosynthesis, providing an essential precursor for auxin
498 biosynthesis and thus promoting auxin production [43]. JOX2 is a JA-inducible dioxygenase
499 that converts the active defense hormone JA into biologically inactive 12-hydroxy-JA
500 (12-OH-JA). This oxidative inactivation limits excessive JA accumulation and contributes to
501 the balance between plant defense and growth[44]. In this study, the JA-related genes *JAZ8*,
502 *JAZ10*, and *JOX2*, together with the auxin biosynthesis-associated gene *TRPA1*, were
503 significantly downregulated in the Yellow module. These findings suggest that Pro-Ca may
504 modulate vegetative growth via multiple targets at the early stage. Downregulation of *JAZ*

genes may relieve repression of JA signaling, while reduced *TRPA1* expression could attenuate auxin biosynthesis; these changes in JA and auxin pathways may collectively contribute to the suppression of vegetative vigor.

Structural wall components such as lignin and cellulose can accumulate in the primary and secondary cell walls of vascular tissues, increasing stem rigidity[45]. At the mid-stage (10-15 d) of treatment, DEGs showed significant enrichment in the MAPK signaling pathway and the plant-pathogen interaction pathway, suggesting that defense and oxidative stress responses accompanied growth inhibition. At 10 d, enriched terms concerned glucan metabolism (including cellulose and hemicellulose) and xyloglucan transferase activity, whereas at 15 d, enrichment involved cell wall biosynthesis-related pathways such as secondary cell wall biogenesis. These results suggest that alterations in cell wall synthesis and degradation are associated with Pro-Ca-mediated shoot growth suppression at the mid-stage. Here, significant enrichment of DEGs in cell-wall-metabolism-related pathways was consistent with previous observations that Pro-Ca increased cortical parenchyma cell-wall thickness[25, 46], suggesting a possible role in promoting cell-wall deposition. Many NAC family transcription factors promote plant growth and increase stress resistance [47-49], and also regulate secondary cell wall biosynthesis and lignin metabolism in plants. These factors respond to phytohormone signals and regulate cell wall remodeling and lignification in herbaceous and woody horticultural species[50-54]. FLA11 has been shown to act as a cell wall surface sensor that detects mechanical signals, regulates secondary cell wall development, and balances lignin and cellulose synthesis and deposition in the secondary cell wall[55, 56]. RIC4 promotes cortical microfilament cytoskeleton assembly, which drives cell protrusion and outward growth, and positively regulates plant growth[57, 58]. In this study, *NAC37*, *FLA11*, and *RIC4* in the magenta module exhibited high intramodular connectivity and were identified as core candidate genes. Combined with functional annotations and published evidence, these three

genes are speculated to be cooperatively involved in Pro-Ca-induced cell wall remodeling and lignification, thereby participating in the regulatory response of peach shoot growth. Notably, these functional correlations are inferred merely from transcriptomic co-expression patterns. Since cell wall component contents and structural parameters were not determined in the present study, the precise regulatory mechanism remains to be further validated. The present transcriptomic results are consistent with previous reports that Pro-Ca promotes lignin accumulation and enhances stem rigidity in pepper [13]. At 20 d post-treatment, DEG numbers peaked among the four time points. Enrichment was observed for DNA replication, DNA repair, anthocyanin biosynthesis and ABA signaling pathways. These results suggest that Pro-Ca's inhibitory effect was attenuated, and plants began to resume vegetative growth alongside DNA replication activation.

Together, these results suggest that Pro-Ca regulates excessive shoot growth in greenhouse-grown peach through processes beyond inhibition of the gibberellin pathway, with early hormonal signaling responses, mid-stage regulation of cell wall lignification, and late-stage compensatory transcriptional activation. The findings extend our understanding of Pro-Ca regulation in peach and provide transcriptomic evidence to guide the development of safe and efficient shoot control strategies for greenhouse cultivation. However, gene expression changes in this study were assessed solely using transcriptomic data. Future work should combine physiological measurements of endogenous hormone contents, cell wall components, and stem mechanical properties with functional validation of candidate genes such as *NAC37* and *JAZ8*, to clarify the specific contributions of these candidate genes to peach shoot growth regulation.

Conclusions

This study examined the spatiotemporal basis of shoot growth regulation by Pro-Ca in greenhouse peach. Among the concentrations tested, 400 mg/L was optimal for suppressing

excessive shoot elongation, increasing leaf chlorophyll content, and improving fruit flavor. The results implicate multi-hormonal cross-talk, regulation of the JA–auxin signaling balance, and cell wall remodeling associated with lignification in Pro-Ca-mediated shoot growth inhibition. These findings extend understanding of Pro-Ca action in fruit trees and provide a theoretical basis for its use in greenhouse peach production.

Declarations

Data Availability Statement

The raw sequencing data generated in this study have been deposited in the NCBI Sequence Read Archive (SRA) database under accession number PRJNA1556277. A reviewer access link:https://dataview.ncbi.nlm.nih.gov/object/PRJNA1556277?reviewer=cnci9dkpcha6ld7kcqu675n2oj. The data will be released publicly upon acceptance of this manuscript.

Conflicts of Interests

The authors declare that they have no competing interests.

Funding

This work was funded by the Fundamental Research Funds for Hebei Academy of Agriculture and Forestry Sciences(No.2025020102), the earmarked fund for Hebei Agriculture Research System (HARS)(No.HBCT2024160205) and the earmarked fund for China Agriculture Research System (No.CARS-30-Z-02).

Authors' contributions

YW, Conceptualization. YW, ZYW, YHL, JL, RFC, QHT, Data curation. YW, Formal analysis. YW, ZYW, YHL, JL, GJL, QHT, ZDT, Investigation. ZYW, YHL, JL, RFC, GJL, Methodology. ZYW, Project administration. ZYW, YHL, QHT, Resources. YW, Visualization. YW, ZYW, YHL, JL, GJL, QHT, Writing – original draft. YW, ZYW, YHL, RFC, ZDT, Writing – review & editing.

Acknowledgements

Not applicable.

References

1. Sun P, Zhu W, Lin X, Wu J, Cao Y, Chen C, Wang Y, Zhu J, Jia H, Qian M *et al*: **Effects of rainy and low light conditions on coloration and flavonoid accumulation in peach peel based on metabolomic and transcriptomic analyses**. *Sci Agric Sin* 2025, **58**(6):1173-1194.
2. Thomidis T, Zioziou E, Koundouras S, Navrozidis I, Nikolaou N: **Effect of prohexadione-Ca on leaf chlorophyll content, gas exchange, berry size and composition, wine quality and disease susceptibility in Vitis vinifera L. cv Xinomavro**. *Scientia Horticulturae* 2018, **238**:369-374.
3. Rademacher W: **Growth retardants: effects on gibberellins biosynthesis and other metabolic pathways**. *Annual Review of Plant Physiology and Plant Molecular Biology* 2000, **51**(1):501-531.
4. Liu H, Xu Y, Wang Y, Liu C, Chen J, Fan S, Xie L, Dong Y, Chen S, Zhou W *et al*: **Study on endocrine disruption effect of paclobutrazol and uniconazole on the thyroid of male and female rats based on lipidomics**. *Ecotoxicology and Environmental Safety* 2022, **234**:113386.
5. Evans JR, Evans RR, Regusci CL, Rademacher W: **Mode of Action, Metabolism, and Uptake of BAS 125W, Prohexadione-calcium**. *HortScience* 1999, **34**(7):1200-1201.
6. Wang H, Yu X, Tang J, Zhao Q, Yang R, Bai J, Cao L, Xiong R: **Effects of Prohexadione Calcium on Lodging Resistance and Yield in High-Quality japonica Rice**. *Agronomy* 2026, **16**(10):974.
7. Duong MV, Chung J-W, Ha VG, Moon H, Yu J-K, So Y-S: **Prohexadione-Calcium Mitigates the Overgrowth of Corn Seedlings**. *Agronomy* 2024, **14**(2):371.

8. Carra B, Pasa MS, Fachinello JC, Spagnol D, Abreu ES, Giovanaz MA: **Prohexadione calcium affects shoot growth, but not yield components, of 'Le Conte' pear in warm-winter climate conditions**. *Scientia Horticulturae* 2016, **209**:241-248.

9. Musacchi S, Sheick R, Mia MJ, Serra S: **Studies on physiological and productive effects of multi-leader training systems and Prohexadione-Ca applications on apple cultivar 'WA 38'**. *Scientia Horticulturae* 2023, **312**:111850.

10. Medjdoub R, Val J, Blanco A: **Prohexadione–Ca inhibits vegetative growth of 'Smoothee Golden Delicious' apple trees**. *Scientia Horticulturae* 2004, **101**(3):243-253.

11. Cline JA, Embree CG, Hebb J, Nichols DS: **Performance of prohexadione-calcium on shoot growth and fruit quality of apple-Effect of spray surfactants**. *Canadian Journal of Plant Science* 2008, **88**(1):165-174.

12. Kim HM, Lee HR, Kang JH, Hwang SJ: **Prohexadione-Calcium Application during Vegetative Growth Affects Growth of Mother Plants, Runners, and Runner Plants of Maehyang Strawberry**. *Agronomy* 2019, **9**(3):155.

13. Xia K, Hu P, Wu G, He X, Li Y, Li Y, Wang F, Cui D, Li S: **Prohexadione calcium boosts pepper stem rigidity: coordinated regulation of hormonal crosstalk and lignin deposition drives xylem reinforcement**. *BMC Plant Biology* 2025, **25**(1):1225.

14. Li D, Yang J, Dai Z, Chen Y, Shao Z, Wang C, Jin X, Wang Y, Feng L: **Prohexadione-calcium improves grape quality by regulating endogenous hormones, sugar and acid metabolism and related enzyme activities in grape berries**. *BMC Plant Biology* 2024, **24**(1):122.

15. Chang P-T: **Influence of Prohexadione-Calcium on the Growth and Quality of Summer 'Jen-Ju Bar' Guava Fruit**. *Journal of Plant Growth Regulation* 2016, **35**(4):980-986.

16. Kanehisa M, Furumichi M, Sato Y, Matsuura Y, Ishiguro-Watanabe M: **KEGG for characterizing genomes and pathways in the biosphere**. *Nucleic Acids Research* 2026:gkag1042.

17. Kanehisa MA-OX, Furumichi M, Sato Y, Matsuura Y, Ishiguro-Watanabe M: **KEGG: biological systems database as a model of the real world**. *Nucleic Acids Research* 2025, **53**:D672-D677.

18. Kanehisa M: **Toward understanding the origin and evolution of cellular organisms**. *Protein Science* 2019, **28**:1947-1951.

19. Kanehisa M, Goto S: **KEGG: kyoto encyclopedia of genes and genomes**. *Nucleic Acids Research* 2000, **28**:27-30.

20. Medjdoub R, Val J, Blanco A: **Physiological effects of prohexadione-calcium in apple trees: effects on parameters related to photoproductivity**. *J Hortic Sci Biotechnol* 2007, **82**(1):126-132.

21. Sabatini E, Noferini M, Fiori G, Grappadelli LC, Costa G: **Prohexadione-Ca positively affects gas exchanges and chlorophyll content of apple and pear trees**. *European Journal of Horticultural Science* 2003, **68**(3):123-128.

22. Mondal TK, Li Y, Zhou H, Feng N, Zheng D, Ma G, Feng S, Liu M, Yu M, Huang X *et al*: **Physiological and transcriptome analysis reveals that prohexadione-calcium promotes rice seedling's development under salt stress by regulating antioxidant processes and photosynthesis**. *Plos One* 2023, **18**(6).

23. Sugar D, Elfving DC, Mielke EA: **Effects of Prohexadione-Calcium on Fruit Size and Return Bloom in Pear**. *HortScience* 2004, **39**(6):1305-1308.

24. Deng R, Zheng D, Feng N, Khan A, Zhang J, Sun Z, Li J, Xiong J, Ding L, Yang X *et al*: **Prohexadione Calcium Improves Rice Yield Under Salt Stress by Regulating Source–Sink Relationships During the Filling Period**. *Plants* 2025, **14**(2):211.

25. McGrath MJ, Koczan JM, Kennelly MM, Sundin GW: **Evidence that Prohexadione-Calcium Induces Structural Resistance to Fire Blight Infection**. *Phytopathology®* 2009, **99**(5):591-596.

26. Saptari RT, Esyanti RR, Putranto RA: **Growth and Steviol Glycoside Content of Stevia rebaudiana Bertoni in the Thin-Layer Liquid Culture Treated with Late-Stage Gibberellin Biosynthesis Inhibitors**. *Sugar Tech* 2020, **22**(1):179-190.

27. Yamaguchi S: **Gibberellin Metabolism and its Regulation**. *Annual Review of Plant Biology* 2008, **59**(1):225-251.

28. Thomas SG, Phillips AL, Hedden P: **Molecular cloning and functional expression of gibberellin 2- oxidases, multifunctional enzymes involved in gibberellin deactivation**. *Proceedings of the National Academy of Sciences* 1999, **96**(8):4698-4703.

29. Sabir IA, Manzoor MA, Shah IH, Abbas F, Liu X, Fiaz S, Shah AN, Jiu S, Wang J, Abdullah M *et al*: **Evolutionary and Integrative Analysis of Gibberellin-Dioxygenase Gene Family and Their Expression Profile in Three Rosaceae Genomes (F. vesca, P. mume, and P. avium) Under Phytohormone Stress**. *Frontiers in Plant Science* 2022, **13**:942969.

30. Hedden P, Thomas Stephen G: **Gibberellin biosynthesis and its regulation**. *Biochemical Journal* 2012, **444**(1):11-25.

31. Jin G, Qi J, Zu H, Liu S, Gershenzon J, Lou Y, Baldwin IT, Li R: **Jasmonate-mediated gibberellin catabolism constrains growth during herbivore attack in rice**. *The Plant Cell* 2023, **35**(10):3828-3844.

32. Li L, Chen X: **Auxin regulation on crop: from mechanisms to opportunities in soybean breeding**. *Molecular Breeding* 2023, **43**(3):16.

33. Zhang C, Li H, Xi D, Huang K, Zhong Y, Luo H, Pei J, Ruan R: **Analysis of the optimal application time of prohexadione calcium and its physiological effects on**

the growth regulation of new shoots of sweet cherry. *J Fruit Sci* 2026, **43**(4):849-862.

34. Andrade Júnior RB, Zanrosso A, Baldissera S, Felix Dias A, Ribeiro JD, Tamiris Canossa A, Gris T, Holtrup Wolff R, Petry Rufato D, Dalazen Machado B *et al*: **Optimizing Vegetative Growth and Yield in Apple Trees Through Split Applications of Prohexadione–Calcium, Ethephon, and NAA**. *Agriculture* 2026, **16**(13):1378.

35. Lal M, Sood Y, Singh H, Kumar A, Wani A, Kumar S: **Influence of prohexadione-calcium on temperate fruit crops – A Review**. *Ecology Environment and Conservation* 2022, **28**:164-172.

36. Zhong W, Deng P, Feng N, Zheng D, Du Y, Deng R, Sun Z, Duan S, Yang X, Yue N: **Integrated transcriptomic and metabolomic analysis of prohexadione calcium-mediated alleviation of salt stress in oilseed rape (*Brassica napus* L.) seedlings**. *BMC Plant Biology* 2026, **26**(1):904.

37. Yang DL, Yao J, Mei CS, Tong XH, Zeng LJ, Li Q, Xiao LT, Sun Tp, Li J, Deng XW *et al*: **Plant hormone jasmonate prioritizes defense over growth by interfering with gibberellin signaling cascade**. *Proc Natl Acad Sci USA* 2012, **109**(19):E1192-E1200.

38. Hou X, Lee LYC, Xia K, Yan Y, Yu H: **DELLAs Modulate Jasmonate Signaling via Competitive Binding to JAZs**. *Developmental Cell* 2010, **19**(6):884-894.

39. Chen Q, Sun J, Zhai Q, Zhou W, Qi L, Xu L, Wang B, Chen R, Jiang H, Qi J *et al*: **The Basic Helix-Loop-Helix Transcription Factor MYC2 Directly Represses PLETHORA Expression during Jasmonate-Mediated Modulation of the Root Stem Cell Niche in Arabidopsis**. *The Plant Cell* 2011, **23**(9):3335-3352.

40. Uji Y, Taniguchi S, Tamaoki D, Shishido H, Akimitsu K, Gomi K: **Overexpression of *OsMYC2* Results in the Up-Regulation of Early JA-Rresponsive Genes and**

Bacterial Blight Resistance in Rice. *Plant and Cell Physiology* 2016, **57**(9):1814-1827.

41. Sui J, Yin Q, Chen Y, Sun M, Yuan X, Ding Z, Kong X: **ERF114/115/109 are essential for jasmonate-repressed non-canonical JAZ8 activity in JA signaling**. *Cell Reports* 2025, **44**(1):115222.

42. Fu W, Jin G, Jiménez-Alemán GH, Wang X, Song J, Li S, Lou Y, Li R: **The jasmonic acid-amino acid conjugates JA-Val and JA-Leu are involved in rice resistance to herbivores**. *Plant, Cell & Environment* 2022, **45**(1):262-272.

43. Bajguz A, Piotrowska-Niczyporuk A: **Biosynthetic Pathways of Hormones in Plants**. *Metabolites* 2023, **13**(8):884.

44. Zhang X, Wang D, Elberse J, Qi L, Shi W, Peng Y-L, Schuurink RC, Van den Ackerveken G, Liu J: **Structure-guided analysis of Arabidopsis JASMONATE-INDUCED OXYGENASE (JOX) 2 reveals key residues for recognition of jasmonic acid substrate by plant JOXs**. *Molecular Plant* 2021, **14**(5):820-828.

45. Ma D, Ding Y, Liu Y, Du L, Mo Y, Dai A, Xu J, Gu D, Duan L, Tan W: **Optimizing application strategies of prohexadione-calcium·uniconazole composite regulator to improve lodging resistance and grain yield in rice cultivation in East China**. *Field Crops Research* 2025, **328**:109931.

46. Wallis AE, and Cox, K. D.: **Management of fire blight using pre-bloom application of prohexadione-calcium**. *Plant Disease* 2020, **104**(4):1048–1054.

47. Srivastava R, Kobayashi Y, Koyama H, Sahoo L: **Overexpression of cowpea NAC transcription factors promoted growth and stress tolerance by boosting photosynthetic activity in Arabidopsis**. *Plant Science* 2022, **319**:111251.

48. Masri R, Kiss E: **The role of NAC genes in response to biotic stresses in plants**. *Physiological and Molecular Plant Pathology* 2023, **126**:102034.

49. Yu L, Asghar MA, Petridis A, Xu F: **Unlocking Dendrobium officinale‘s drought resistance: Insights from transcriptomic analysis and enhanced drought tolerance in tomato**. *J Integr Agric* 2025, **24**(11):4282-4293.

50. Li X: **Mining and FunctionalAnalysis of NAC Transcription Factors Related to Juice Sacs Granulation of 'Sanhongmiyou'**. *Doctoral Degree.* FujianAgriculture and Forestry University; 2021.

51. Li X, Huang H, Rizwan HM, Wang N, Jiang J, She W, Zheng G, Pan H, Guo Z, Pan D *et al*: **Transcriptome Analysis Reveals Candidate Lignin-Related Genes and Transcription Factors during Fruit Development in Pomelo (Citrus maxima)**. *Genes* 2022, **13**(5):845.

52. Li X, Wang N, She W, Guo Z, Pan H, Yu Y, Ye J, Pan D, Pan T: **Identification and Functional Analysis of the CgNAC043 Gene Involved in Lignin Synthesis from Citrusgrandis “San Hong”**. *Plants* 2022, **11**(3):403.

53. Xu Q, Wang W, Zeng J, Zhang J, Grierson D, Li X, Yin X, Chen K: **A NAC transcription factor, EjNAC1, affects lignification of loquat fruit by regulating lignin**. *Postharvest Biology and Technology* 2015, **102**:25-31.

54. Zhong R, Demura T, Ye Z-H: **SND1, a NAC Domain Transcription Factor, Is a Key Regulator of Secondary Wall Synthesis in Fibers of Arabidopsis**. *The Plant Cell* 2006, **18**(11):3158-3170.

55. Ma Y, MacMillan CP, de Vries L, Mansfield SD, Hao P, Ratcliffe J, Bacic A, Johnson KL: **FLA11 and FLA12 glycoproteins fine-tune stem secondary wall properties in response to mechanical stresses**. *New Phytologist* 2022, **233**(4):1750-1767.

56. MacMillan CP, Mansfield SD, Stachurski ZH, Evans R, Southerton SG: **Fasciclin-like arabinogalactan proteins: specialization for stem biomechanics and cell wall architecture in Arabidopsis and Eucalyptus**. *The Plant Journal* 2010, **62**(4):689-703.

754 57. García-González J, Havelková L, Bellinvia E, Corrales I, Pejchar P, Potocký M,
755 Schwarzerová K: **Independent roles of Arp2/3 complex and RIC4 protein in the**
756 **control of epidermal cell shape**. *Planta* 2026, **263**(4):110.
757 58. Lin D, Ren H, Fu Y: **ROP GTPase-mediated auxin signaling regulates pavement**
758 **cell interdigitation in Arabidopsis thaliana**. *Journal of Integrative Plant Biology*
759 2014, **57**(1):31-39.
760

Supplementary Files

This is a list of supplementary files associated with this preprint. Click to download.

- Table1.pdf
- FigS1.pdf